Applied Surface Science 539 (2021) 148259

Contents lists available at ScienceDirect

Applied Surface Science

journal homepage: www.elsevier.com/locate/apsusc

Mechanisms of molecular emission from phenylalanine monolayer deposited on free-standing graphene bombarded by C_{60} projectiles

Mikołaj Gołuński, Sviatoslav Hrabar, Zbigniew Postawa *

Smoluchowski Institute of Physics, Jagiellonian University, ul. Lojasiewicza 11, 30-348 Krakow, Poland

ARTICLE INFO

Keywords:
MD simulations
SIMS
Graphene
Organic overlayer
Sputtering
C60

ABSTRACT

The Molecular Dynamics (MD) computer simulations are used to gain insight into the mechanism of molecular ejection from a monolayer of phenylalanine ($C_9H_{11}NO_2$) molecules deposited on free-standing two-layer graphene. The system is bombarded with C_{60} projectiles with different kinetic energy and angle of incidence. Mass spectra, sputtering yields, and angular distributions of emitted particles are recorded in two bombardment geometries, in which the projectile hits the sample from above and below.

The sputtering yields increase with the primary kinetic energy. There is an optimal angle of incidence for each kinetic energy, leading to the most effective molecular emission. The value of this angle increases with kinetic energy. The interplay between the area energized by the impinging projectile, the energy back-reflection, and molecular fragmentation determines the shape of the yield dependence on the angle of incidence. The bombardment geometry has little effect on the efficiency of molecular emission. Generally, organic molecules are emitted by interaction with the projectile and/or a graphene substrate. The main factor affecting the relative contribution of each of these interactions is whether graphene is punctured. The implications of current results for the potential use of graphene supports in Secondary Ion Mass Spectrometry are discussed.

1. Introduction

In recent years, cluster ion beams have attracted increasing experimental and theoretical attention due to their ability to increase the ejection of large intact organic molecules and reduce the accumulation of chemical damage in Secondary Ion Mass Spectrometry (SIMS) [1–4]. The use of cluster projectiles enabled three-dimensional depth profiling of organic and biological systems, exposing this technique to the universe of new possibilities. One of the most successful clusters used in organic SIMS is C_{60} fullerene [5]. In standard SIMS geometry, the detector is on the same side of the target as the ion gun. Usually, metals or semiconductors are used to support the investigated material. Recently, a novel SIMS configuration has been proposed, using transmission orientation in combination with free-standing graphene support [6]. In this orientation, the analyzed organic material is deposited on one side of the ultra-thin substrate, while cluster projectiles bombard another side. The use of ultra-thin support allows for minimizing interference between substrate and analyte signals. The formation of negative molecular ions is also increased by two orders of magnitude due to the presence of graphene [7–9]. It was therefore argued that such geometry could be particularly attractive for studying isolated small nano-objects and supramolecular assemblies [6–10].

There is an extensive database of theoretical studies aimed at determining processes leading to the emission of molecules deposited on thick substrates [1,11–19]. In particular, it was found that various processes are responsible for molecular ejection, depending on whether the projectile is atomic or cluster [1]. For atomic projectiles, the development of a linear collision cascade leads to particle emission [20]. Simultaneous interactions with many ejecting substrate atoms are necessary to stimulate the uplifting of large organic molecules having multiple contact points with the surface [12]. The probability that monoatomic projectiles will generate a time and space-correlated ejection of a sufficient number of substrate atoms to displace a large organic molecule sharply decreases as the number of these contact points increases. As a result, these projectiles are not optimal for the uplifting of large intact molecules.

Much better are cluster projectiles. The impact of these projectiles leads to the development of a non-linear collision cascade and the

* Corresponding author.
E-mail addresses: mikolaj.golunski@doctoral.if.uj.edu.pl (M. Gołuński), sviatoslav.hrabar@doctoral.uj.edu.pl (S. Hrabar), zbigniew.postawa@uj.edu.pl (Z. Postawa).

https://doi.org/10.1016/j.apsusc.2020.148259
Received 21 May 2020; Received in revised form 15 October 2020; Accepted 22 October 2020
Available online 28 October 2020
0169-4332/© 2020 Elsevier B.V. All rights reserved.

unfolding of the topmost layers in a time and space correlated manner [21–23]. The formation of a crater is one of the consequences of this action. Another consequence is the ejection of organic molecules by the collective processes [14,15]. For large gas cluster projectiles, the molecules can also be entrained in a stream of projectile atoms reflected from the substrate [17–19]. This process is particularly effective in the case of off-normal impacts of projectiles consisting of thousands of weakly bonded atoms. It should be noted that simulations of bulk phenylalanine sample bombardment with large gas clusters confirm the "gas-flow" mechanic with the emission of intact molecules mainly from the rim of the crater [24]. Finally, small, weakly bound molecules can be uplifted from the substrate by interacting with circular acoustic waves [13,16]. Such waves can be generated by cluster impacts on the surface of materials with a membrane-like structure, like graphite.

Although the molecular emission from the organic overlayers deposited on thick substrates is well documented, much less is known about the processes leading to molecular emission from two-dimensional (2D) substrates. Processes generated in such substrates must be different due to their limited vertical dimensions, which does not allow for the development of a full collision cascade. Several simulations have been performed on the C_{60} bombardment of clean graphene [6,25–31]. So far, only a few simulations of the C_{60} bombardment of organic molecules deposited on free-standing graphene have been performed [8,9,32]. All these simulations are performed for impacts in transmission geometry. Moreover, they are limited to the normal incidence and minimal range of incident kinetic energy. There is no simulation studying molecular emission from graphene bombarded by cluster projectiles in standard sputtering configuration, in which both the ion gun and the detector are on the same side of the substrate. The purpose of this article is to investigate the processes that lead to the ejection of organic molecules deposited on ultrathin free-standing graphene utilizing a wide range of projectile kinetic energies and impact angles. Molecular emission stimulated by projectile impacts conducted in the novel transmission configuration and standard sputtering setup is investigated to identify and explain differences in mechanisms of molecular emission in these two systems. The implications of the results for the potential use of graphene support in Secondary Ion Mass Spectrometry are discussed.

2. Material and methods

The molecular dynamics (MD) computer simulations are used to model cluster bombardment. Briefly, the movement of particles is determined by integrating Hamilton's equations of motion. The forces between carbon atoms in the system are described by the ReaxFF-lg force field [33], which allows for the formation and breaking of covalent bonds. This potential is splined at short distances with a Ziegler-Biersack-Littmark (ZBL) potential [34] to describe high-energy collisions adequately. We have decided to use the ReaxFF-lg potential as it was made for modeling energetic collisions. It should be pointed out, however, that a Reax potential parametrized to describe the amino acids is also published [35]. This potential was parametrized to describe low-energy processes. Therefore, it should be supplemented with a repulsive wall to accurately describe interatomic collisions at short distances (high-energy collisions). We have run a series of trial simulations with both potentials and found out that in our system, the results are similar. We have already published a few studies aimed to investigate various aspects of the particle emission from clean graphene and graphene covered with phenylalanine molecules using the Reax-lg potential [25,26,32]. Therefore, this force-field will be used in this manuscript to allow for a direct comparison of the current and previously published data. However, it should be stressed that parametrization developed for amino acids should be used in sputtering studies, where low-energy collisions are responsible for particle emission. Such a situation will occur, for example, during cluster bombardment of bulk phenylalanine systems. In this case, a full collision cascade will develop inside a thick sample, and the particles emitted into the vacuum will originate from a low-energy tail of this cascade [20]. Electronic stopping was disregarded as in the case of the investigated sample and energies the nuclear stopping is much more prevalent than electronic processes [34]. A more detailed description of the MD method can be found elsewhere [1].

The shape and size of the samples are selected on the basis of visual observations of energy transfer pathways stimulated by C_{60} impacts [25,26]. As a result, cylindrical samples with a diameter of 40 nm are used. We observe that for the smaller sample (35 nm), the sample size affects the results. On the other hand, using a sample with a diameter of 45 nm makes the simulations more computationally intensive, with no added benefit. The samples consist of a double layer of graphene with a highly oriented pyrolytic graphite structure. We produced a HOPG structure by creating ideal graphene sheets in AB stacking and minimizing their energy. We confirmed the structure by visual inspection of a stable graphene sample. The whole sample consists of a single graphene "crystal". We used a double layer of graphene due to our previous collaboration with an experimental group that operated on such a system and required a theoretical analysis of their experimental outcomes [6–10]. Therefore, our current results can be related to these studies. Moreover, such substrates can be easily purchased, giving opportunities for other experimenters to verify our work. A monolayer of phenylalanine molecules ($C_9H_{11}NO_2$) is deposited on graphene. Molecules were first placed on the graphene surface in an orderly fashion with an experimental density of Phe monolayer [36]. Then their positions have been randomized, and the energy of the whole sample has been minimized through prolonged simulation with no constraints. Phenylalanine was chosen because it is an essential amino acid that enables research into the system of interest to the bio-SIMS community. The molecule is also relatively simple, which reduces the computational cost of calculations. The thickness of the organic monolayer (without graphene) is about 1 nm. The samples are bombarded by C_{60} projectiles directed at the graphene substrate (transmission geometry) or the organic layer (sputtering geometry), as shown in Fig. 1. A wide range of kinetic energies (0.5–40 keV) and the incidence angles (0°–80°) of the projectile are used to investigate the influence of these parameters on the particle ejection process. The angle of incidence is defined between the direction of the initial projectile motion and the normal vector of the sample plane. Organic particles ejected from both sides of the sample are collected. However, there is almost no emission of organic material into the "substrate side" of the graphene sheet, even with impacts conducted in sputtering geometry (Fig. 1). Therefore, only the emission of particles on the "organic side" of the sample is discussed later in the paper.

Rigid and stochastic regions are used to simulate a thermal bath that maintains the sample at the required temperature, to prevent reflection

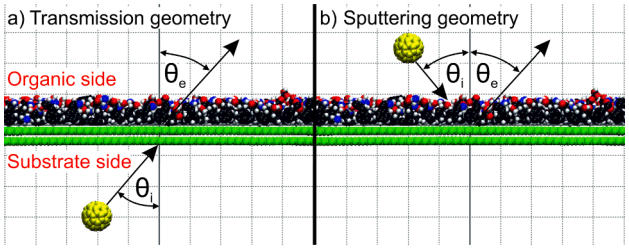

Fig. 1. Schematic diagram of systems used to model C_{60} bombardment of phenylalanine monolayer deposited on free-standing graphene in a) transmission and b) sputtering geometry. C_{60} projectile atoms are yellow, graphene atoms are green, while atoms of organic molecules are expressed by following colours: carbon is black, nitrogen is blue, oxygen is red, hydrogen is grey. The arrows indicate the directions of the projectile impact and the emission of material from the sample. The polar emission angle and the angle of projectile incidence are marked by θ_e and θ_i, respectively. The polar angles larger than zero are referred to as "off-normal polar angles". (For interpretation of the references to colour in this figure legend, the reader is referred to the web version of this article.)

of pressure waves from the boundaries of the system, and to maintain the shape of the sample [23]. These boundaries are proposed originally for 3D solids, and their application to 2D systems is not apparent. To test the applicability of such an approach, we performed calculations for a series of 10 keV C_{60} impacts at a clean 2-layer graphene substrate that was 8 times larger (320 nm diameter) than the original system used in our study. This system's size was large enough to ensure that even the quickest disturbances induced by the projectile impact did not reach the system's boundaries within the time needed to complete the emission of all particles. As a result, there is no effect of the rigid and stochastic boundaries on the sputtering yield in such a system. Within the statistical accuracy of our results, we do not see any difference in the sputtering yields calculated on both systems, which proves the applicability of the adopted approach to 2D systems, at least for analysis of the particle ejection process. The simulations are run at a target temperature of 0 K. They extend to 20 ps for impacts with kinetic energy below 15 keV, and 40 ps otherwise. This time is sufficient to achieve saturation of the ejection yield versus time dependence. For each set of conditions, nine impacts are simulated at randomly selected points located near the center of the sample to obtain statistically reliable data. Simulations are performed with the large-scale atomic/molecular massively parallel simulator code (LAMMPS) [37] that has been modified to model sputtering conditions more efficiently.

3. Results

We start by examining the effect of primary kinetic energy and the angle of incidence on the movement of the C_{60} projectile atoms. Such knowledge is useful for determining graphene piercing conditions and the efficiency of the primary energy deposition process. The number of projectile atoms penetrating and back-reflecting from the sample and the fraction of the primary kinetic energy lost by these atoms during interaction with the bombarded system is presented in Fig. 2. Let's start by examining the effect of projectile kinetic energy for impacts along normal to the surface. For kinetic energy less than or equal to 1 keV, none of the projectile atoms penetrate the sample. However, even if the sample is not raptured, the projectile loses a significant portion of its primary kinetic energy. For example, for kinetic energy below 5 keV, almost all energy is transferred from the projectile to the bombarded system. Also, the number of back-reflected projectile atoms is minimal, which indicates that most of the projectiles are trapped at the sample. The transmitted projectile atoms emerge for 2 keV C_{60} impacts, which indicates that the sample is ruptured. The number of transmitted projectile atoms increases as the primary kinetic energy increases until all projectile atoms pass through the sample. At the same time, a smaller portion of the projectile kinetic energy is deposited in the sample. For example, almost 90% of the impact energy is deposited in the system by 5 keV C_{60}. This value drops to just 40% for the system bombarded by 40 keV projectile. There is no difference in the efficiency of the energy deposition process for impacts conducted in transmission and sputtering configuration. However, the number of transmitted projectile atoms is sensitive to bombardment geometry, especially near the energy needed to pierce the sample. Fewer projectile atoms pass through the sample during impacts that occur near surface normal in sputtering configuration than transmission geometry.

The angle of incidence also has an apparent effect on the number of transmitted and back-reflected projectile atoms and the amount of energy transferred from the projectile to the system. The number of transmitted projectile atoms decreases as the angle of incidence increases when the kinetic energy of the projectile is constant. Most of the atoms that do not penetrate the sample are back-reflected, especially for off-normal impacts. Projectile atoms can also be trapped inside the sample. The probability of this process increases with the increase of the angle of incidence and reduction of kinetic energy. For each primary kinetic energy, there is a critical angle when none of the projectile atoms penetrate the sample. The value of this angle increases with the primary

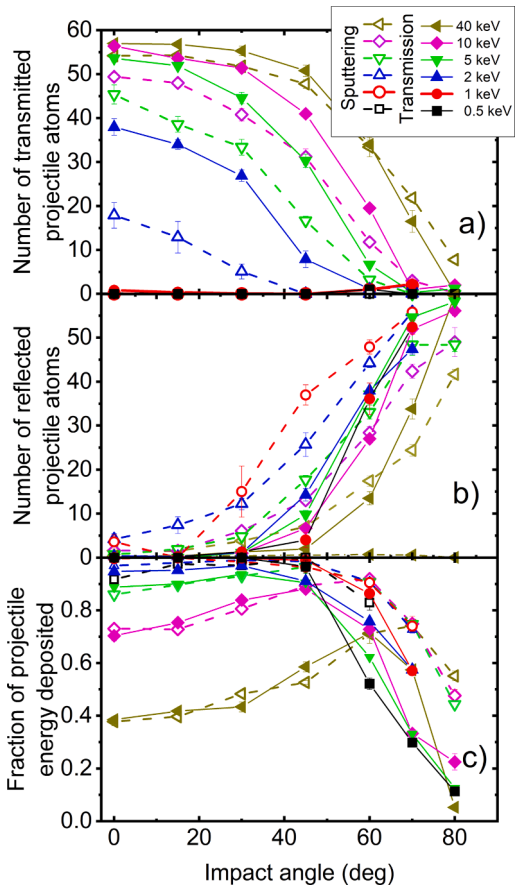

Fig. 2. Dependence of the number of projectile atoms a) transmitted through the sample and b) reflected from the sample and c) a fraction of the projectile's primary kinetic energy deposited in the sample on the kinetic energy and angle of incidence of C_{60} projectile bombarding the sample in sputtering (open symbols and dashed lines) and transmission geometry (full symbols and solid lines). Vertical lines with whiskers denote error bars resulting from multiple impacts simulated for each set of initial conditions, as described in Section 2.

kinetic energy. The angle of incidence also affects the efficiency of energy losses. This effect is especially visible in the case of high energy impacts. Initially, this amount increases with the angle of incidence, as shown in Fig. 2c. In the end, however, the amount of energy transferred to the system decreases as more energy is back-reflected. The shape of the dependence of the number of transmitted projectile atoms on the angle of incidence is similar for transmission and sputtering geometry. Impact geometry also has little effect on the amount of energy loss, at least for angles of incidence below 60°. At larger angles, more energy is transferred to the sample during impacts in the sputtering geometry.

Knowledge about what happens to projectile atoms provides useful information about the behavior of the bombarded system. However, for the potential use of graphene in SIMS, knowledge about the emission of organic molecules is much more important. The mass spectra of the particles emitted from the phenylalanine overlayer bombarded with 0.5 keV, 10 keV, and 40 keV C_{60} projectiles at normal incidence are presented in Fig. 3. The spectra only show particles ejected from the organic overlayer, i.e., both the projectile and graphene atoms are eliminated from this figure. The peak corresponding to the intact phenylalanine molecules occurs in all spectra. The height of this peak is comparable in almost all cases presented in Fig. 3. Only for 0.5 keV C_{60} impact, conducted in sputtering configuration, the emission of intact molecules hardly exists. However, this behavior is expected because this projectile has very low kinetic energy. The presence of strong emission of intact molecules for 0.5 keV C_{60} bombardment in transmission geometry is much more mysterious. For all presented impacts, the emission of intact

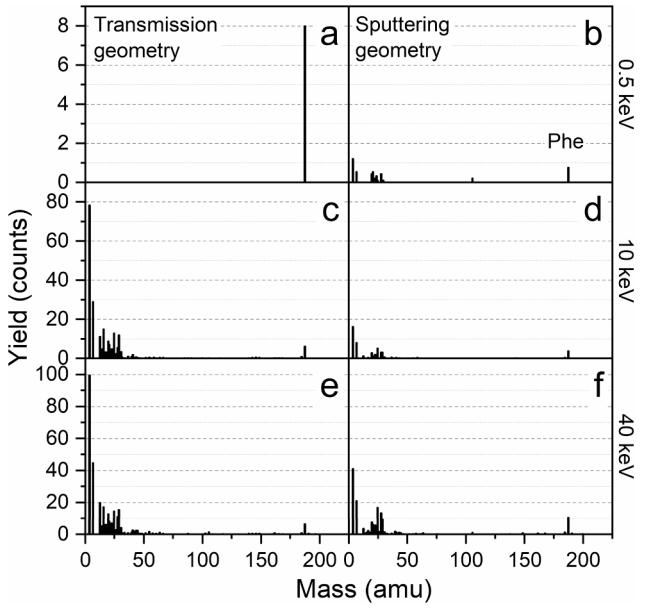

Fig. 3. Mass spectra of particles emitted from the phenylalanine (Phe) overlayer by a, b) 0.5 keV, c, d) 10 keV and e, f) 40 keV C_{60} projectile impacts in transmission (left panel) and sputtering (right panel) geometry. In all cases projectiles arrive at the sample along the surface normal. Dashed lines in the background are for reference only.

molecules is accompanied by the ejection of molecular fragments. The most abundant are H atoms, followed by H_2, C_2, O, and C.

Analysis of the mass spectra allows determining how the projectile properties affect the degree of fragmentation and emission efficiency of the analyzed molecules. This knowledge is necessary, for example, to find optimal ion-beam settings leading to the most efficient emission of intact molecules. Having a strong signal of the intact molecule is a significant concern for SIMS. The impact of the primary kinetic energy and angle of incidence on the number of ejected intact phenylalanine molecules and their fragments is presented in Fig. 4. Data for molecular fragments are expressed in molecular equivalents. In this representation, the given point represents the total mass of all emitted fragments divided by the mass of the intact phenylalanine molecule. The shapes of all graphs are similar. For each primary kinetic energy, there is a specific local angle of impact that leads to the most abundant ejection of particles, which we call an optimal impact angle θ_e^{opt}. The value of this angle depends on the primary kinetic energy and impact configuration, as shown in the insets. For 0.5 keV C_{60} impacts conducted in transmission configuration, the strongest ejection occurs when the sample is bombarded along a surface normal. In this case, the yield monotonically decreases as the angle of incidence increases. The most abundant emission shifts towards higher angles of incidence as the primary kinetic energy increases (see insets to Fig. 4). On the other hand, for sputtering geometry, the maximum emission always occurs at the off-normal angles of incidence. Similar behavior is observed for molecular fragments. The number of fragments decreases as the kinetic energy of the projectile decreases, which is anticipated because collisions become more gentle for projectiles with lower energy.

The results presented in Fig. 4 lead to two unexpected conclusions. First, fragmentation of the molecules is more critical in transmission than in sputtering geometry. The basic process leading to the formation of fragments are direct collisions with projectile atoms [3,11,14,38]. More energetic collisions should occur in sputtering geometry, where the projectile collides with an organic overlayer, still having its original kinetic energy. For transmission geometry, a significant part of the kinetic energy is lost during graphene perforation [26]. As a result, less energetic collisions should occur between the projectile and organic molecules, which should lead to less fragmentation. This behavior clearly does not take place. It is also surprising that there is no gain in the material emission yield when transmission geometry is used instead of a standard sputtering configuration. One of the reasons for proposing this innovative configuration was the expectation that the projectile bombarding the sample from below would lead to a stronger emission of organic material. In this arrangement, the projectile momentum is transferred directly to the molecules of the organic layer, and the molecules eject directly towards the detector. In the sputtering configuration, the projectile momentum transferred to organic molecules must first be reverted. One would expect this process to be less effective. Contrary to these expectations, molecular yields are comparable in both geometries. Only when the sample is not raptured, the emission of intact molecules is higher in transmission geometry.

The ejection yield is one of the key parameters for the efficient detection of the analyzed material. However, the directionality of emission is also important. The kinetic energy integrated polar angle distributions of intact molecules ejected by projectile impacts are shown in Fig. 5. The data in this figure are also azimuthally integrated and peak-normalized. Only for 0.5 keV and 1 keV projectile impacts conducted in the transmission configuration intact molecules are ejected near the surface normal. For all other impacts, the most effective ejection of these species occurs at the off-normal polar angles, usually around 50°.

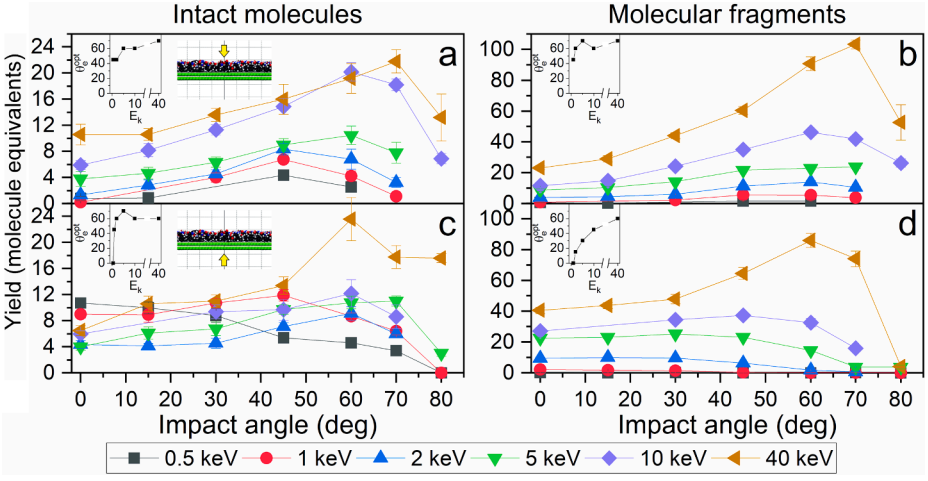

Fig. 4. Dependence of the yield on intact molecules (a, c) and molecular fragments (b, d) on the kinetic energy and angle of incidence of C_{60} projectiles. The particles are emitted from a monolayer of phenylalanine molecules deposited on graphene bombarded by C_{60} projectiles from above (a, b) and below (c, d), as indicated by the yellow arrows in the insets. The inset diagrams represent the dependence of the polar angle leading to the most efficient emission, θ_e^{opt}, on the projectile kinetic energy E_k. (For interpretation of the references to colour in this figure legend, the reader is referred to the web version of this article.)

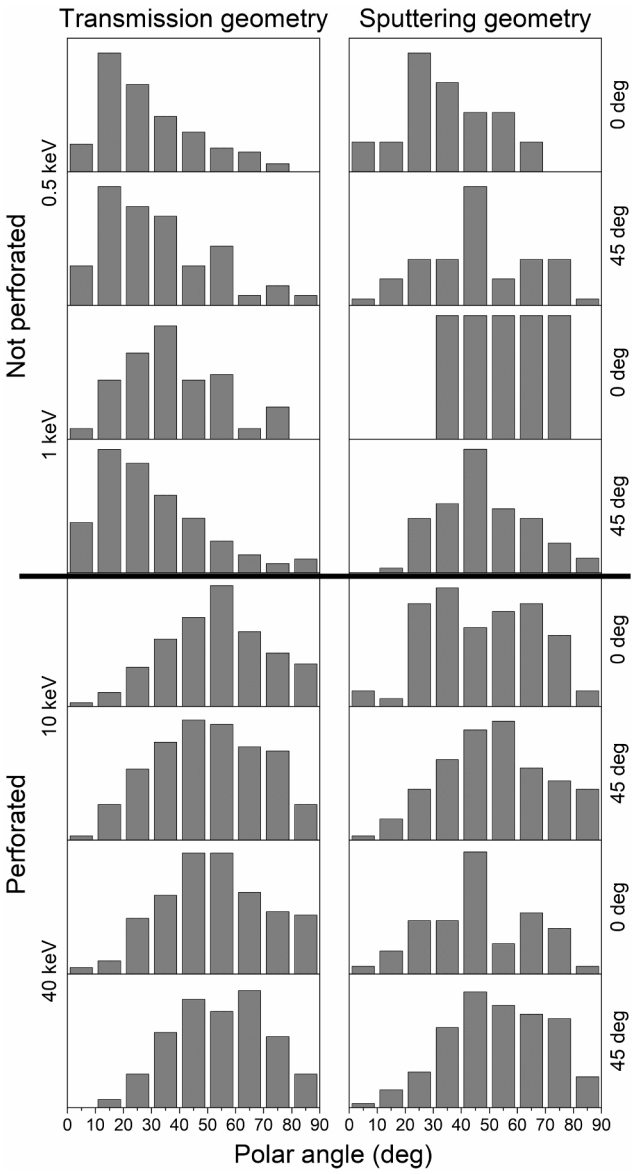

Fig. 5. Peak-normalized angular distributions of intact phenylalanine molecules ejected after C_{60} impacts with a different kinetic energy and angle of incidence.

4. Discussion

Processes responsible for the particle ejection should be delineated to explain observed trends. This task can be accomplished by performing a mechanistic analysis of energy transfer pathways, tracking the temporal evolution of the system. Such an evolution is shown in Fig. 6 for the impacts of 0.5 and 10 keV C_{60} projectiles along the surface normal. These two energies are selected to represent low- and high-energy impacts, i.e., impacts that do not cause perforation of the sample or lead to a puncture. These impacts are also visualized in Animations 1, 2, 3, and 4. Analysis of this data indicates that the main factor differentiating the mechanisms of molecular ejection is whether the sample has been punctured or not.

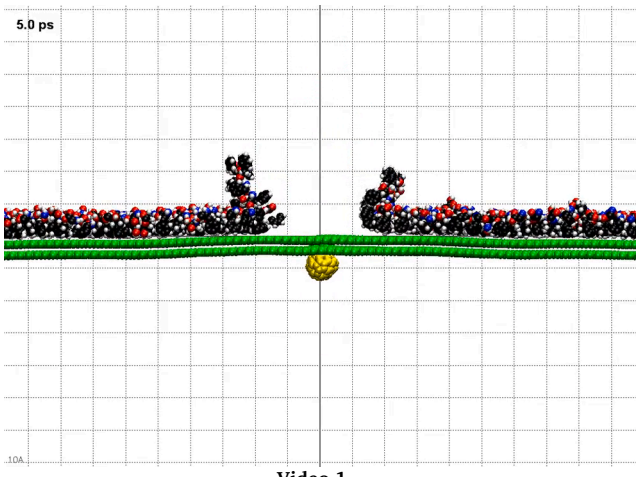

Video 1.

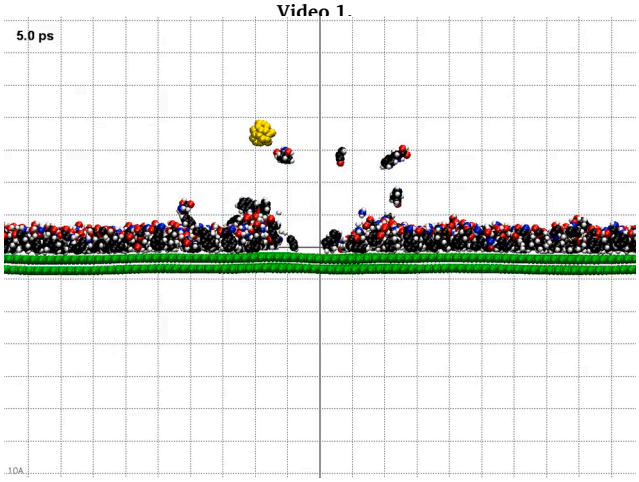

Video 2.

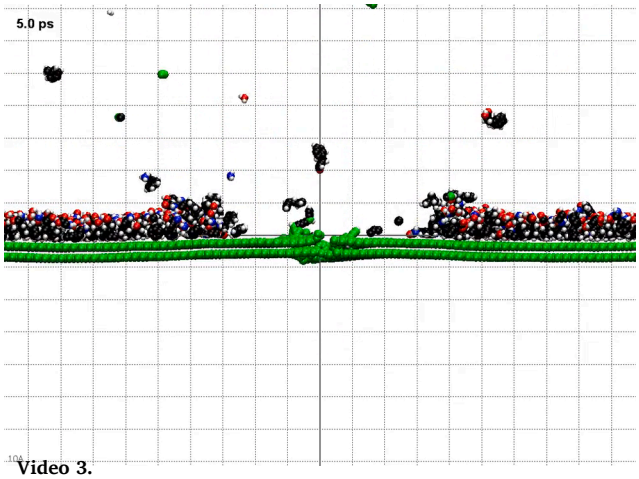

Video 3.

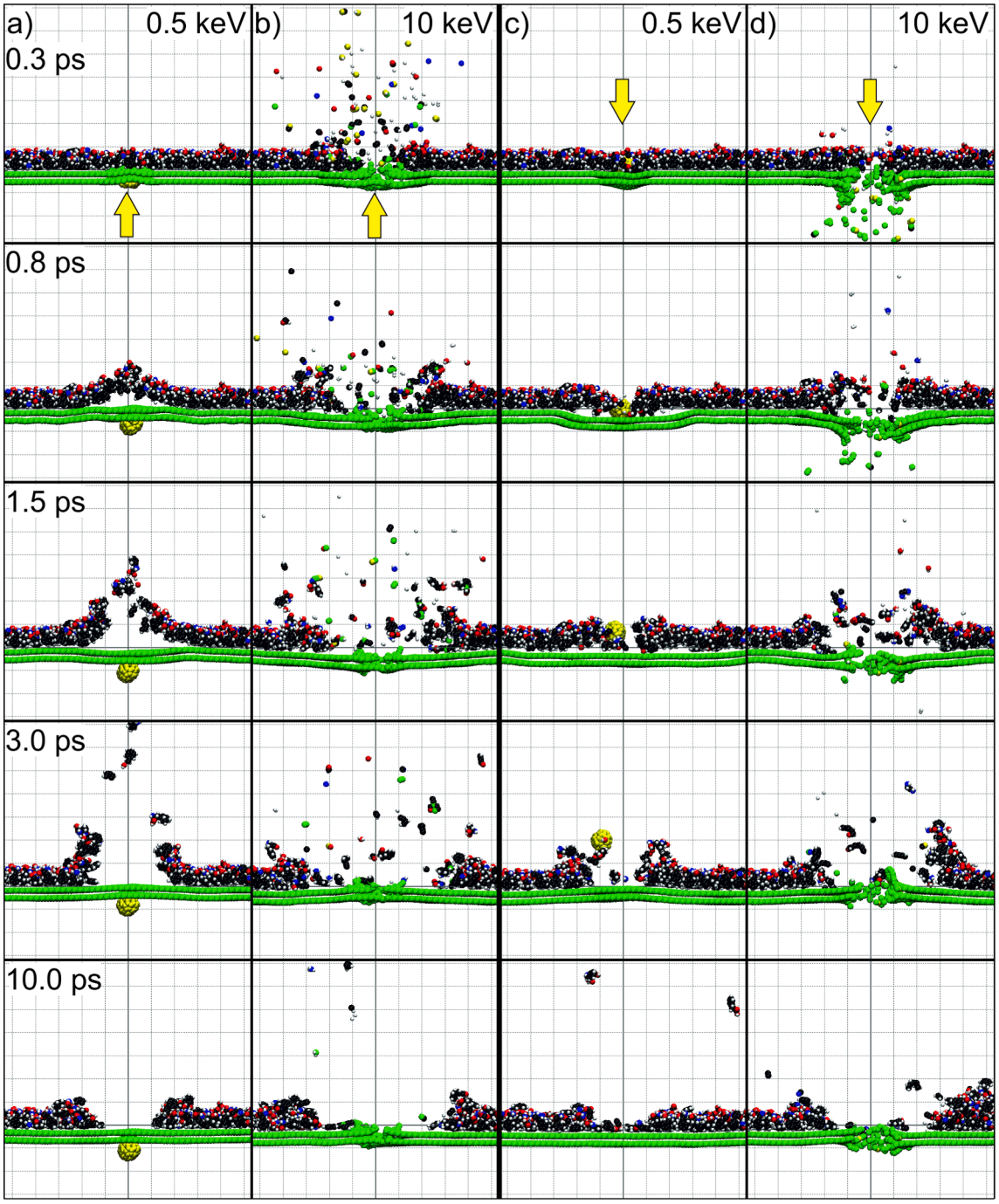

Fig. 6. Temporal snapshots from the simulation of 0.5 keV and 10 keV C_{60} impacts of C_{60} projectile along the surface normal at phenylalanine monolayer deposited on free-standing graphene. Only 2 nm wide slice through the centre of the sample is shown. Thin lines in the background denote the distance of 1 nm. The yellow arrows indicate directions of the projectile impact. (For interpretation of the references to colour in this figure legend, the reader is referred to the web version of this article.)

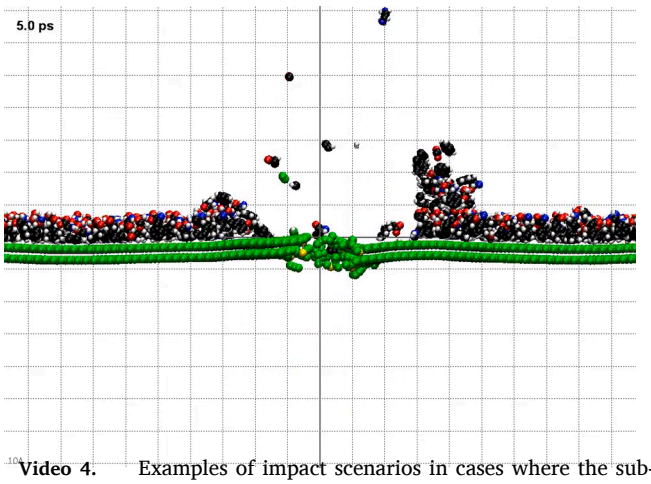

Video 4. Examples of impact scenarios in cases where the substrate is not perforated are shown in Fig. 6a and c for 0.5 keV C_{60} bombardment conducted in transmission and sputtering geometry, respectively. These impacts are also visualized in Animations 1 and 3. In both cases, the integrity of the projectile is not compromised upon the impact. It interacts with a surrounding environment as one object, though its structure can get disturbed after impact, especially during high-angle impacts. For transmission geometry, the projectile collides directly only with the graphene substrate. Graphene sheets bulge out along the direction of the primary beam, pushing organic molecules up. The process is delicate and spatially correlated. As a result, molecular fragmentation is minimal. About 0.6 ps after impact, a portion of the organic layer near the impact point detaches from the substrate. About 0.8 ps, the projectile stops completely, and graphene layers begin to return to their original shape. However, molecules previously energized by graphene deformation are no longer in contact with the substrate. They continue to move up. These molecules are only bound to the sample by intermolecular forces. These forces are too weak to prevent molecules from leaving the sample. The ejected molecules move mainly in directions close to the normal to the surface. Finally, small circular acoustic waves are generated in the substrate. They propagate away from the point of impact energizing molecules further away. However, the energy of these waves is too low to uplift phenylalanine molecules. Eventually, all movement in the system disappears, and the projectile remains trapped at the bottom of the graphene substrate.

For bombardment conducted in sputtering geometry, the projectile comes from above the sample. First, it interacts with the molecules of the organic layer, pushing them aside. Also, in this case, the projectile is not destroyed and transfers its kinetic energy to neighboring molecules in a delicate way. However, now its kinetic energy is higher than during impacts in transmission geometry, where some of the projectile energy was absorbed by graphene. As a consequence, molecular fragmentation, although small, is more pronounced than in the case of bombardment in transmission geometry, as shown in Fig. 3. After passing through the overlayer, C_{60} comes in contact with graphene, pushing it down. Initially, the organic overlayer remains flat. As a result, the gap between the molecules and the substrate is formed near the point of impact. At about 0.7 ps, the organic molecules begin to follow the downward motion of graphene. The movement of the molecules is slow. At about 1.1 ps, deformed graphene begins to straighten under the influence of elastic strain forces. However, it must take another 1 ps before the molecules start moving up. In the meanwhile, acoustic waves are generated in graphene. These waves dissipate the deposited energy from the impact zone. The straightening layers of graphene act like a catapult trying to throw molecules into a vacuum. However, most of the energy deposited in the impact zone is already taken away by the waves. As a result, the sputtering yield is very low, as shown in Fig. 3. Intact molecules are emitted at off-normal polar angles because they have already obtained some transverse momentum when the projectile has penetrated the layer. Eventually, the emission of particles stops.

Different ejection scenarios occur in cases where the kinetic energy of the projectile is sufficient to pierce the sample. Examples of such impact scenarios are shown in Fig. 6b and d for 10 keV C_{60} bombardment carried out in transmission and sputtering geometry, respectively. These impacts are also visualized in Animations 2 and 4. For the high-energy bombardment, differences between impacts conducted in transmission and sputtering geometry are much smaller than in cases where the sample was not punctured. After the projectile impact, the sample is quickly perforated, and an almost circular rupture forms in the sample. For transmission geometry, the projectile breaks down when it collides with graphene. It is no longer a single object. Instead, it creates a conglomerate of smaller particles moving independently. This conglomerate also contains particles ejected from the graphene substrate. All these particles move with high kinetic energy. Their movement is no longer correlated spatially and temporally. They collide with organic molecules located near the point of impact, shattering them into pieces. As a result, all molecules located within a circular zone with a diameter of approximately 2 nm, centered at the projectile point of impact, are destroyed. The emission of organic particles starts already at 0.1 ps. Initially, only molecular fragments are emitted as a result of direct interaction with the energetic projectile, and substrate particles are emitted. Most of these fragments move in a direction close to the normal to the surface.

For sputtering geometry, the projectile first collides with the organic overlayer. Its kinetic energy is higher than in the case of the transmission configuration, in which part of the energy is consumed for graphene perforation. However, projectile integrity is not yet compromised by contact with the organic layer. The projectile disintegrates only after hitting graphene. For now, it still interacts with organic molecules as a single large object. Although the projectile kinetic energy is high, the collisions between projectile and organic molecules are spatially and temporally correlated. As a result, they are more gentle, and fewer molecules are destroyed. Thus, the difference in the projectile integrity during interaction with the sample is responsible for the smaller fragmentation observed in sputtering than transmission geometry, which was unexpected.

For both incidence geometries, the transmitted and knocked-on atoms carry some of the projectile kinetic energy. Another part of this energy is deposited in graphene near the rupture rim. Graphene sheets start to move vigorously in this area. An energized zone is also created in the organic overlayer. It undergoes lateral expansion. An almost planar pressure wave is generated in the organic layer, which leads to the collective movement of phenylalanine molecules. The pressure wave also relocates organic molecules away from the point of impact, forcing some of them to pile up. As a result, these particles form a circular rim around the zone cleared of molecules, and the disturbed area of the organic overlayer extends far beyond the area of the crack formed in graphene. The weak binding of phenylalanine molecules to the graphene substrate and inside the overlayer facilitates this phenomenon.

The critical process that regulates the abundance of the ejecta is the separation of the molecular layer from graphene. The downward movement of graphene leads to this separation. For transmission geometry, radial compression of the molecular layer pushes the graphene membrane down. For sputtering configuration, graphene is pushed down mainly by interaction with the incoming projectile. The propagation of the pressure pulse in the organic layer in combination with layer/substrate separation leads to the bending of the organic layer upwards and the emission of molecules. This emission is additionally stimulated by correlated interaction with the graphene substrate. Membrane atoms interact with atoms of phenylalanine molecules and transfer the momenta to them. In this way, the molecules eject without destruction. In other words, the membrane acts like a trampoline for molecules [8,9]. The energetics of the above processes is similar in both tested impact geometries. Accordingly, particle emission is comparable

in both cases.

The temporal evolution of the system bombarded by 0.5 keV and 10 keV C_{60} impacts at 45° is shown in Fig. 7. It is also visualized in Animations 5, 6, 7, and 8. A comparison of these data with the data shown in Figs. 2 and 6 leads to the conclusion that three factors should be considered in order to accurately describe changes in molecular emission due to the change of the angle of incidence. The first factor is related to the area of the sample excited by the projectile. As the angle of incidence increases, the projectile can move a longer path inside the organic layer. As a consequence, it can collide with a more significant number of organic molecules and uplift them. This phenomenon enhances molecular emission and is essential for low-energy impacts, non-perforating the sample, conducted in sputtering geometry. It is also crucial for high-energy impacts rupturing the sample. It is not essential for low-energy impacts in the transmission configuration because the projectile cannot immerse in the organic layer. The second factor is related to the component of the projectile momentum perpendicular to the sample and projectile back-reflection process. For off-normal impacts, this component is reduced. Moreover, an increasing part of projectile kinetic energy is carried by back-reflected projectile atoms for off-normal impacts, as shown in Fig. 2. Consequently, less energy is available to stimulate molecular emissions. This phenomenon reduces molecular emission. The third process is related to molecular fragmentation. In cases where an increase in the angle of incidence

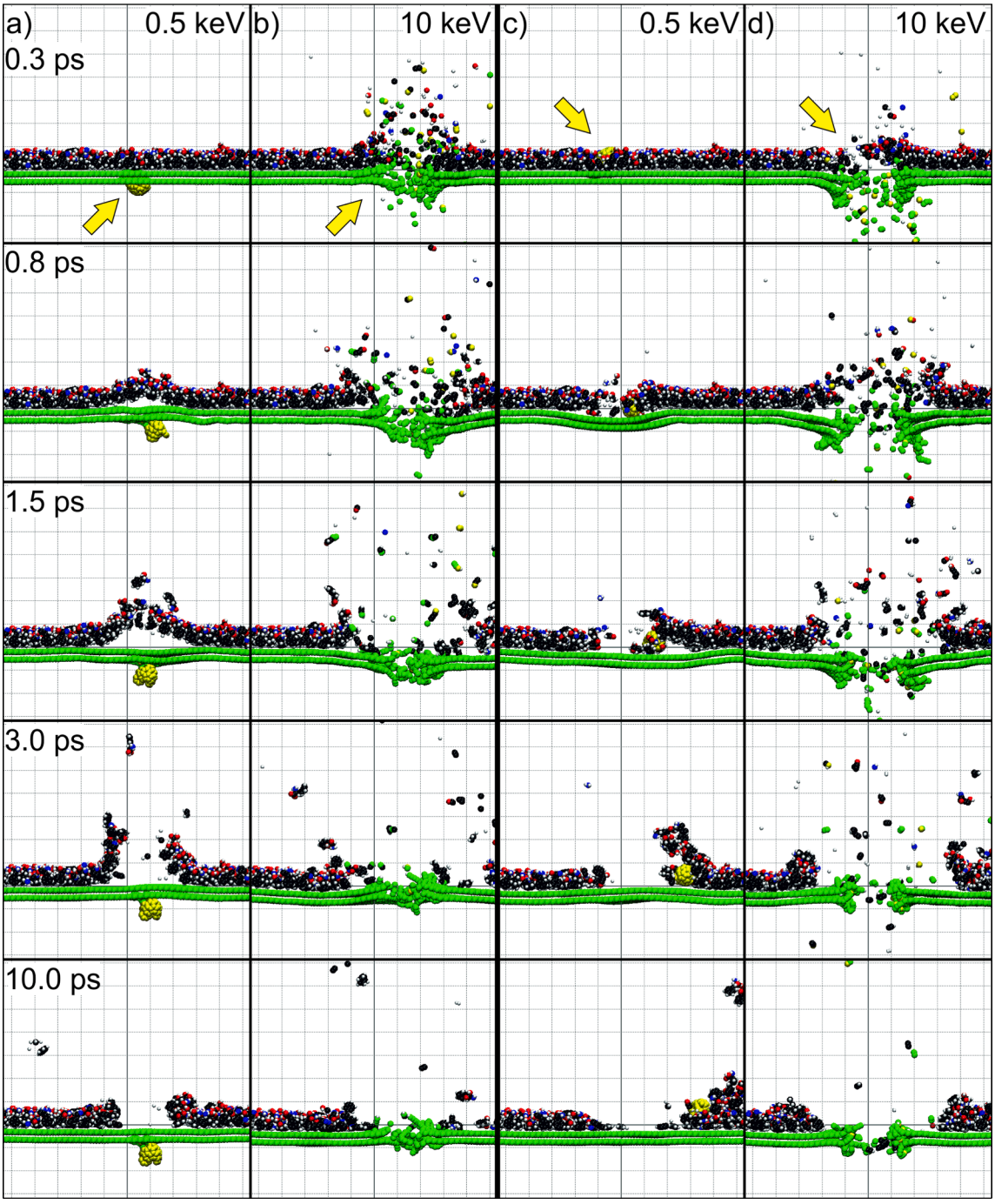

Fig. 7. Temporal snapshots from the simulation of 0.5 keV and 10 keV C_{60} impacts at phenylalanine monolayer deposited on free-standing graphene at 45° incidence angle. A detailed description of the content of the figure is provided in Fig. 6.

makes collisions less energetic, fewer molecules are fragmented. As a result, the yield of intact molecules increases at the expense of the yield of molecular fragments. This situation can occur because, in the case of off-normal impacts, some of the energy is reflected back.

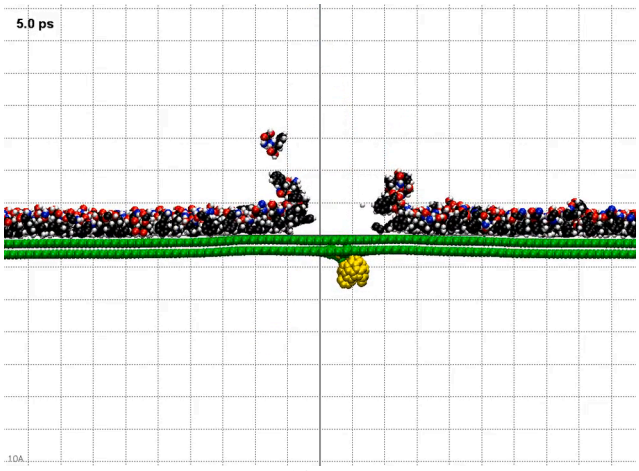

Video 5.

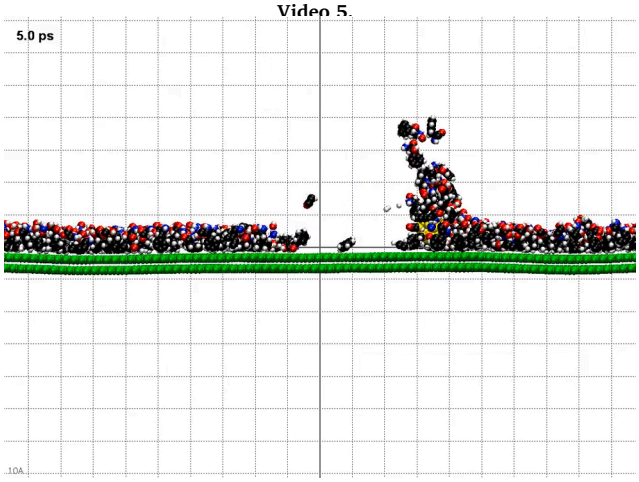

Video 6.

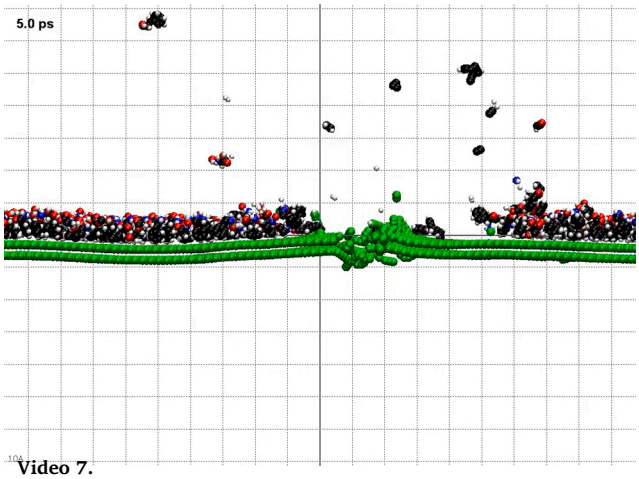

Video 7.

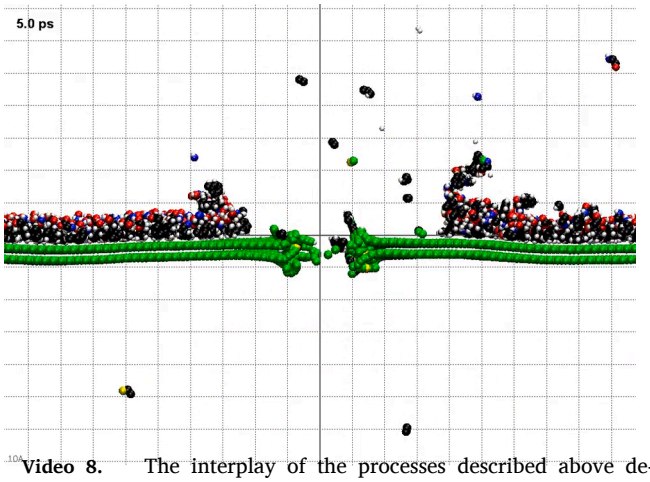

Video 8. The interplay of the processes described above determines the shape of the yield versus impact angle dependence. For example, for high-energy impacts, the first process initially dominates, and the signals of intact molecules and fragments increase. At a certain angle of incidence, the decrease in the energy available for the molecular emission overweights the increase in the emission area and the signal decreases. An increase of the projectile kinetic energy reduces the impact of energy back-reflection, as seen in Fig. 2, and consequently, shifts the angle corresponding to the maximum signal to a higher value. The influence of the third process is especially visible in the case of high-energy impacts at high impact angles in transmission geometry. It is, for example, responsible for keeping strong molecular emission for 40 keV C_{60} impacts at 80°. For low-energy impacts, the fragmentation is already minimal. For low-energy impacts conducted in transmission geometry, the influence of the first process also is minimal. In this case, the projectile just bounces off graphene and has no contact with the organic layer. Consequently, the signal decreases as the angle of incidence increases because less energy is available to bulge the substrate and stimulate molecular ejection. It is noteworthy that in the case of low-energy impacts in transmission geometry, only the momentum component perpendicular to the sample appears to be responsible for molecular ejection. This conclusion is based on the observation that even in the case of off-normal impacts, intact molecules are still ejected close to the surface normal, as shown in Fig. 7a.

The data presented in Fig. 2 indicate that the bombardment process in transmission and sputtering geometry may not be symmetrical. The difference between these two impact geometries becomes especially visible in the case of impacts with kinetic energy close to the threshold energy needed to rupture the sample. The results obtained on a clean two-layer graphene system bombarded with C_{60} projectiles at normal incidence show that about 63%, 46%, and 20% of the projectile kinetic energy is deposited in this sample by 5 keV, 10 keV, and 40 keV C_{60}, respectively [26]. After conversion into energy units, the energy deposited in the sample is 3.1 keV, 4.5 keV, and 8 keV, respectively. The data presented in Fig. 2c indicate that the analogous values obtained for the current system are approximately 85%, 70%, and 35% or 4.3 keV, 7 keV, and 14 keV. A comparison of these numbers indicates that graphene is the main absorber of deposited energy, especially during low-energy impacts. In transmission geometry, the projectile collides with graphene with original kinetic energy. The energy of the projectile in contact with graphene in sputtering geometry is lower because some of the energy is already lost in the organic overlayer. As a result, fewer projectile atoms have a chance to penetrate through graphene in sputtering setup than in transmission geometry. For high-energy impacts, projectile atoms coming into contact with graphene in transmission and sputtering geometry also have different kinetic energy. In this case, however, the projectiles have excess kinetic energy, which makes it possible to penetrate the sample, regardless of impact geometry.

5. Conclusions

The effect of the kinetic energy, angle of incidence, and geometry of the projectile impact on the efficiency of particle ejection from phenylalanine monolayer deposited on free-standing graphene is investigated. It has been found that the signal increases with the primary kinetic energy. However, more energetic impacts also lead to more significant molecular fragmentation. For a given kinetic energy, there is a specific angle of incidence, which leads to the most efficient molecular emission. This angle increases with the increase of the projectile kinetic energy. The interplay of three factors determines the shape of the relationship between the yield and the angle of incidence. The first factor is related to the area of the sample energized by the projectile. With the increase of the angle of incidence, the projectile may travel a longer path inside the organic layer or energize a larger area of a graphene substrate. Consequently, it can collide with and uplift a larger number of phenylalanine molecules. The second factor is related to the component of the projectile momentum perpendicular to the sample and the process of projectile back-reflection. For off-normal impacts, this component is reduced, and an increasing part of projectile kinetic energy is dissipated by the back-reflected projectile atoms. Consequently, less energy is available to stimulate molecular emissions. The third factor is related to molecular fragmentation. In cases where the increase of the incidence angle makes collisions less energetic, fewer molecules are fragmented. As a result, the yield of intact molecules may increase at the expense of the yield of molecular fragments.

The mechanism of molecular emission from phenylalanine monolayer deposited on free-standing graphene bombarded by keV C_{60} projectile bombardment are delineated. In general, molecules are emitted by interaction with the projectile atoms and graphene substrate. The main factor influencing the relative contribution of each of these two phenomena is whether graphene is punctured. In the case that graphene is not punctured and the projectile arrives from below the sample (transmission geometry), the direct interaction between the substrate and adsorbed molecules is the only process that leads to particle emission. The projectile interacts directly only with graphene, leading to its deformation. The kinetic energy accumulated in this deformation is subsequently transferred to the molecules. The ejection of intact molecules is significant in this case, and the molecules are emitted near the surface normal. If a projectile bombards the organic side of the sample (sputtering geometry), the direct energy transfer between the projectile and the organic molecules is entirely responsible for molecular emission. Graphene plays the role of a non-penetrable membrane, redirecting projectile momentum upwards. Also, in this case, mainly intact molecules are emitted, but the emission is very low. Impact geometry has a significant impact on the effectiveness of molecular emission for bombardment along the surface normal. A robust molecular signal is present in transmission geometry, while the emission is very low for the sputtering configuration. However, this difference decreases with the angle of incidence, and, for example, at 45°, the yields measured in transmission and sputtering geometries are comparable.

In the event of impacts leading to the sample perforation, organic particles are emitted through the joint action of projectile atoms and a graphene substrate. The projectile kinetic energy deposited in graphene leads to the ejection of substrate atoms and deformations of graphene, especially near the rupture. The first phenomenon leads to the creation of a hole in the substrate and fragmentation of molecules colliding with these particles. Graphene bending acts like a trampoline and ejects weakly bound molecules, especially in transmission geometry. Graphene movement also leads to the temporary separation of the molecular layer from the substrate. Direct collisions between projectile atoms and the organic molecules cause a molecular fragmentation and emission of fragments. However, some of the energy deposited in the organic overlayer also leads to the formation of a planar pressure pulse. This pulse propagates in the overlayer and accelerates the molecules sideways. The process is not very energetic. However, in combination with the temporary separation of molecules from the substrate due to the bending of graphene, it also leads to the emission of molecules. The flux of particles ejected in directions close to the surface normal consists mainly of molecular fragments, while intact molecules are emitted predominantly at off-normal angles. Impact geometry does not affect the efficiency of molecular ejection. We do not see molecular emission stimulated by interaction with the acoustic waves generated in graphene by the projectile impact.

Finally, a few comments on the possibilities of using graphene substrates for SIMS analysis are given. Previous studies have shown that the presence of graphene can increase the efficiency of negative organic ion formation by 2 orders of magnitude [8]. This observation is the basis of the suggestion that graphene would be an excellent substrate for studying isolated small nano-objects and supramolecular assemblies. The proposed mechanisms of ionization involve the tunneling of electrons from the vibrationally excited area around the rupture to the molecules, and/or a direct proton transfer exchange. If someone would only be interested in achieving strong emission of intact neutral molecules, as, in the case of Secondary Neutral Mass Spectrometry (SNMS), the most preferable would be the application of transmission geometry in combination with C_{60} impacts that do not lead to sample perforation. In this case, molecular emission is strong, and there is no chemical damage build up in the bombarded sample. However, SIMS does not register neutral particles, but ions. The probability of ionization will be minimal for low-energy impacts. Higher kinetic energies are needed to ensure effective ionization [8]. Our results indicate that high-energy C_{60} bombardment at off-normal angles is the most preferred configuration for such analyzes because it leads to both high emission and ionization. Our data also show that molecular emission is comparable in transmission and sputtering geometries. This is an important observation because the latter configuration is used in almost all SIMS and other experimental systems using ion beams to analyze and modify materials. As a result, no modification of the experimental system is needed to implement graphene substrates.

CRediT authorship contribution statement

Mikołaj Gołuński: Conceptualization, Formal analysis, Investigation, Methodology, Writing - review & editing, Software, Visualization. **Sviatoslav Hrabar:** Formal analysis, Writing - review & editing, Validation. **Zbigniew Postawa:** Writing - original draft, Supervision.

Declaration of Competing Interest

The authors declare that they have no known competing financial interests or personal relationships that could have appeared to influence the work reported in this paper.

Acknowledgments

The authors gratefully acknowledge financial support from the Polish National Science Center, Programs Nos. 2016/23/N/ST4/00971 and 2019/33/B/ST4/01778. This research was supported in part by PLGrid Infrastructure.

References

[1] B.J. Garrison, Z. Postawa, Computational view of surface based organic mass spectrometry, Mass Spectrom. Rev. 27 (2008) 289–315, and references therein.
[2] N. Winograd, The Development of Secondary Ion Mass Spectrometry (SIMS) for Imaging, in: M.L. Gross, R.M. Caprioli (Eds.), The Encyclopedia of Mass Spectrometry, Elsevier, Boston, 2016, pp. 103–112.
[3] A. Delcorte, B.J. Garrison, K. Hamraoui, Dynamics of molecular impacts on soft materials: from fullerenes to organic nanodrops, Anal. Chem. 81 (2009) 6676–6686.
[4] J.S. Fletcher, Latest applications of 3D ToF-SIMS bio-imaging, Biointerphases 10 (2015) 018902.

[5] D. Weibel, S. Wong, N. Lockyer, P. Blenkinsopp, R. Hill, J.C. Vickerman, A C_{60} primary ion beam system for time of flight secondary ion mass spectrometry: its development and secondary ion yield characteristics, Anal. Chem. 75 (2003) 1754–1764.
[6] S.V. Verkhoturov, S. Geng, B. Czerwinski, A.E. Young, A. Delcorte, E.A. Schweikert, Single impacts of keV fullerene ions on free standing graphene: emission of ions and electrons from confined volume, J. Chem. Phys. 143 (2015) 164302.
[7] S.V. Verkhoturov, B. Czerwinski, D.S. Verkhoturov, S. Geng, A. Delcorte, E. A. Schweikert, Ejection-ionization of molecules from free standing graphene, J. Chem. Phys. 146 (2017) 084308.
[8] S.V. Verkhoturov, M. Golunski, D.S. Verkhoturov, S. Geng, Z. Postawa, E. A. Schweikert, "Trampoline" ejection of organic molecules from graphene and graphite via keV cluster ions impacts, J. Chem. Phys. 148 (2018) 144309.
[9] S.V. Verkhoturov, M. Golunski, D.S. Verkhoturov, B. Czerwinski, M.J. Eller, S. Geng, Z. Postawa, E.A. Schweikert, Hypervelocity cluster ion impacts on free standing graphene: experiment, theory and applications - perspective, J. Chem. Phys. 150 (2019) 160901–160916, and references therein.
[10] S. Geng, S.V. Verkhoturov, M.J. Eller, A.B. Clubb, E.A. Schweikert, Characterization of individual free-standing nano-objects by cluster SIMS in transmission, J. Vac. Sci. Technol. C 34 (2016) 03H117.
[11] R. Chatterjee, Z. Postawa, N. Winograd, B.J. Garrison, Molecular dynamics simulation study of molecular ejection mechanisms: KeV particle bombardment of C6H6/Ag{111}, J. Phys. Chem. B 103 (1999) 151–163.
[12] B.J. Garrison, A. Delcorte, K.D. Krantzman, Molecule liftoff from surfaces, Accounts Chem. Res. 33 (2000) 69–77, and references therein.
[13] M. Kerford, R.P. Webb, Desorption of molecules by cluster impact. A preliminary molecular dynamics study, Nucl. Instrum. Methods Phys. Res. Sect. B: Beam Interactions Mater. Atoms 180 (2001) 44–52.
[14] Z. Postawa, Sputtering simulations of organic overlayers on metal substrates by monoatomic and clusters projectiles, Appl. Surf. Sci. 231 (2004) 22–28.
[15] Z. Postawa, B. Czerwinski, N. Winograd, B.J. Garrison, Microscopic insights into the sputtering of thin organic films on Ag{111} induced by C_{60} and Ga bombardment, J. Phys. Chem. B 109 (2005) 11973–11979.
[16] R.P. Webb, The computer simulation of energetic cluster-solid interactions, Radiat. Eff. Defects Solids 162 (2007) 567–572.
[17] L. Rzeznik, B. Czerwinski, B.J. Garrison, N. Winograd, Z. Postawa, Microscopic insight into the sputtering of thin polystyrene films on Ag{111} induced by large and slow Ar clusters, J. Phys. Chem. C 112 (2008) 521–531.
[18] L. Rzeznik, B. Czerwinski, B.J. Garrison, N. Winograd, Z. Postawa, Molecular dynamics simulations of sputtering of organic overlayers by slow, large clusters, Appl. Surf. Sci. 255 (2008) 841–843.
[19] B. Czerwinski, L. Rzeznik, R. Paruch, B.J. Garrison, Z. Postawa, Effect of impact angle and projectile size on sputtering efficiency of solid benzene investigated by molecular dynamics simulations, Nucl. Instrum. Methods B 269 (2011) 1578–1581.
[20] P. Sigmund, Theory of sputtering. I. Sputtering yield of amorphous and polycrystalline targets, Phys. Rev. 184 (1969) 383–416.
[21] C. Anders, H.M. Urbassek, Cluster-size dependence of ranges of 100eV/atom Au_n clusters, Nucl. Instrum. Methods B 228 (2005) 57–63.
[22] J. Samela, K. Nordlund, Atomistic simulation of the transition from atomistic to macroscopic cratering, Phys. Rev. Lett. 101 (027601) (2008) 027601–027604.
[23] Z. Postawa, B. Czerwinski, M. Szewczyk, E.J. Smiley, N. Winograd, B.J. Garrison, Enhancement of sputtering yields due to C_{60} versus Ga bombardment of Ag{111} as explored by molecular dynamics simulations, Anal. Chem. 75 (2003) 4402–4407.
[24] C. Mucksch, C. Anders, H. Gnaser, H.M. Urbassek, Dynamics of L-phenylalanine sputtering by argon cluster bombardment, J. Phys. Chem. C 118 (2014) 7962–7970.
[25] M. Golunski, Z. Postawa, Effect of sample thickness on carbon ejection from ultrathin graphite bombarded by keV C-60, Acta Phys. Pol. 132 (2017) 222–224.
[26] M. Golunski, Z. Postawa, Effect of kinetic energy and impact angle on carbon ejection from a free-standing graphene bombarded by kilo-electron-volt C-60, J. Vac. Sci. Technol. C 36 (2018) 03F112.
[27] S.J. Zhao, J.M. Xue, L. Liang, Y.G. Wang, S. Yan, Drilling nanopores in graphene with clusters: a molecular dynamics study, J. Phys. Chem. C 116 (2012) 11776–11782.
[28] Z.C. Xu, W.R. Zhong, Probability of self-healing in damaged graphene bombarded by fullerene, Appl. Phys. Lett. 104 (2014) 261907.
[29] J. Luo, T.H. Gao, L. Li, Q. Xie, Z. Tian, Q. Chen, Y.C. Liang, Formation of defects during fullerene bombardment and repair of vacancy defects in graphene, J. Mater. Sci. 54 (2019) 14431–14439.
[30] Z.C. Xu, J.L. Wen, W.R. Zhong, L. Wei, Statistical law of high-energy fullerene and its derivatives passing through graphene, Commun. Theor. Phys. 65 (2016) 361–365.
[31] A.V. Krasheninnikov, F. Banhart, Engineering of nanostructured carbon materials with electron or ion beams, Nat. Mater. 6 (2007) 723–733.
[32] M. Golunski, S.V. Verkhoturov, D.S. Verkhoturov, E.A. Schweikert, Z. Postawa, Effect of substrate thickness on ejection of phenylalanine molecules adsorbed on free-standing graphene bombarded by 10 keV C-60, Nucl. Instrum. Methods B 393 (2017) 13–16.
[33] L.C. Liu, Y. Liu, S.V. Zybin, H. Sun, W.A. Goddard, ReaxFF-lg: correction of the ReaxFF reactive force field for London dispersion, with applications to the equations of state for energetic materials, J. Phys. Chem. A 115 (2011) 11016–11022.
[34] J.F. Ziegler, J.P. Biersack, U. Littmark, The Stopping and Range of Ions in Matter, Pergamon, New York, 1985.
[35] S. Monti, A.C.T. van Duin, S.-Y. Kim, V. Barone, Exploration of the conformational and reactive dynamics of glycine and diglycine on TiO2: computational investigations in the gas phase and in solution, J. Phys. Chem. C 116 (2012) 5141–5150.
[36] A.D. Petelska, M. Naumowicz, Z.A. Figaszewski, The equilibrium of phosphatidylcholine-amino acid system in monolayer at the air/water interface, Cell Biochem. Biophys. 60 (2011) 155–160.
[37] S. Plimpton, Fast parallel algorithms for short-range molecular-dynamics, J. Comput. Phys. 117 (1995) 1–19.
[38] A. Delcorte, B.J. Garrison, keV fullerene interaction with hydrocarbon targets: projectile penetration, damage creation and removal, Nucl. Instrum. Methods B 255 (2007) 223–228.